agronomy

MDPI

Article

Characterization of Biochar Produced in a Mobile Handmade Kiln from Small-Sized Waste Biomass for Agronomic and Climate Change Benefits

Vinicius John [1,2,*], Ana Rita de Oliveira Braga [1,2], Criscian Kellen Amaro de Oliveira Danielli [1,2], Heiriane Martins Sousa [1], Filipe Eduardo Danielli [2,3], Rayanne Oliveira de Araujo [4], Cláudia Saramago de Carvalho Marques-dos-Santos [2], Newton Paulo de Souza Falcão [4] and João Francisco Charrua Guerra [5]

1 Federal Institute of Education, Science, and Technology of Amazonas—IFAM, Manaus 69025-010, AM, Brazil; ana.braga@ifam.edu.br (A.R.d.O.B.); criscian.oliveira@ifam.edu.br (C.K.A.d.O.D.); heiriane.sousa@ifam.edu.br (H.M.S.)
2 Forest Research Centre CEF, Associate Laboratory TERRA, School of Agriculture ISA-UL, University of Lisbon, 1000-001 Lisboa, Portugal; fklauberg@hotmail.com (F.E.D.); cms@isa.ulisboa.pt (C.S.d.C.M.-d.-S.)
3 Superintendency of the Manaus Free Trade Zone—SUFRAMA, Manaus 69075-830, AM, Brazil
4 National Institute for Amazonian Research—INPA, Manaus 69096-000, AM, Brazil; rayannearaujo20@gmail.com (R.O.d.A.); nfalcao@inpa.gov.br (N.P.d.S.F.)
5 Institute of Social Sciences at the University of Lisbon—ICS-UL, University of Lisbon, 1000-001 Lisboa, Portugal; joao.guerra@ics.ulisboa.pt
* Correspondence: vinicius.john@ifam.edu.br

Abstract: Soil amended with biochar is considered a significant response to climate change, remediation of degraded soils, and agronomic improvements. An artisanal mobile pyrolysis kiln was developed for small-sized biomass inputs. Approximately 190 kg of biochar was produced in 21 carbonisation processes using acai residues (*Euterpe oleracea Mart.*) as raw material, as they are among the most abundant agro-industrial residues in the Amazon. It is a valuable and underutilised biomass resource, often inadequately discarded, causing environmental impact and health risks. The physicochemical and structural characteristics of four representative biochar samples from the pyrolysis processes were evaluated using different techniques. The produced biochar had an average pH of 8.8 and the ICP-OES results indicate that the most abundant elements were potassium (K) and phosphorus (P). Results of the elemental composition indicate that the produced biochar has a very stable carbon with an average H/C ratio of 0.23 and O/C ratio of 0.16, indicating that the pyrolysis performed was effective in transforming organic and volatile compounds into stable structures. Variations in nutrient contents call for soil application planning, as performed for other agricultural inputs. The developed mobile kiln can be adapted and favour the decentralisation of biochar production among small and medium-sized producers. Here, we show that even with variations in artisanal production, the biochar produced exhibits favourable characteristics for agronomic use and combating climate changes.

Keywords: biochar; climate change; soil health; agriculture residues; sustainability; low-cost kiln; handmade production

Citation: John, V.; Braga, A.R.d.O.; Danielli, C.K.A.d.O.; Sousa, H.M.; Danielli, F.E.; de Araujo, R.O.; Marques-dos-Santos, C.S.d.C.; Falcão, N.P.d.S.; Guerra, J.F.C. Characterization of Biochar Produced in a Mobile Handmade Kiln from Small-Sized Waste Biomass for Agronomic and Climate Change Benefits. *Agronomy* **2024**, *14*, 1861. https://doi.org/10.3390/agronomy14081861

Academic Editor: Anabel Fernandez

Received: 22 July 2024
Revised: 8 August 2024
Accepted: 16 August 2024
Published: 22 August 2024

1. Introduction

Acai berry is the fruit of an Amazonian palm tree (*Euterpe oleracea Mart.*) considered one of the main products of Brazilian extractivism [1] with an estimated 1.7 million tons produced and sold in 2022, either extracted by wild harvesting and forest management, or cultivation in monocultures and agroforestry systems. Acai berry production is concentrated in the state of Pará, in the Amazon Region, accounting for 90% of this production [2,3].

Acai berry fruit pulp is sold in over 40 countries, with the United States leading the consumer market [4]. Acai berry business is on the rise, due to increasing interest in superfoods, and the energetic and health benefits it provides [5]. In 2022, it was estimated to be USD 1.2 billion, double the amount in 2018 [6].

Currently, only the pulp of the acai berry fruit has commercial value, with 71 to 95% of the extracted fruit wasted [7], and composed of seeds with attached fibres, peels, and pulp remains. Thus, it can be estimated that the annual production of acai berry agro-industrial waste is around 1.2 to 1.6 million tons. It is a valuable yet often wasted resource, occasionally utilised for energy production, but often inappropriately disposed of into the environment, leading to environmental contamination, greenhouse gas emissions, and hazards to human health [8,9]. The simplified biochar production process using acai berry fruit waste as the raw material from agro-industrial sources is presented in Figure 1. The production of biochar carried out in this project began with the acquisition of waste from agro-industries, starting from step 4 in the mentioned figure.

Figure 1. Scheme of biochar production using acai berry fruit waste as raw material, from palm, harvest, agro-industrial processing, waste generation, sieving, drying, and conversion.

Studies have explored different applications for the sustainable management of this relevant agro-industrial waste, such as in the energy sector [10–13], construction [14], pollutant retention [15,16], and biochar production [17,18]. Thermal conversion of acai berry waste can produce a rich and long-lasting biochar capable of sequestering carbon in the soil, due to the lignocellulosic characteristics of its biomass [18,19]. Recent research indicates the use of biochar as a carrier for nanoparticles and also enriched with other substances to enhance electron transfer [20,21]. Moreover, using agro-industrial residues avoids the cultivation of other biomasses that could lead to competition for food production areas as well as the use of other biomasses that may contain contaminants and limit biochar utilisation [22–24].

Internationally, biochar refers to charcoal produced to be applied to soils as a conditioner or for environmental management. But, in the Amazon region, the charcoals were incorporated into the soil from the controlled carbonisation of food remnants and crops over thousands of years by indigenous populations giving way to the formation of the Terra Preta do Índio soil, Amazon dark earth (ADE). Considered as one of the world's most fertile and resilient anthropogenic soils, the addition of biochar to soils seeks to mimic these properties using modern techniques, promoting significant improvements in soils, but still without achieving results similar to Terra Preta [25–30].

Biomasses used for biochar production can be divided according to their origin into wood, agricultural, animal residues, industrial, and aquatic [31], from both rural and urban areas. Pyrolysis is the most commonly used method for biochar production, characterised as a process of thermal decomposition of the organic matrix of biomasses in an oxygen-

restricted environment [32]. The conversion above the thermal stability limit of the biomass forms a more stable product, biochar [24].

Like small Amazonian producers, other countries and regions also have a tradition of using charcoal in agriculture [33]. However, low-cost carbonisation of small-sized agricultural waste biomasses on a viable scale to produce biochar for agricultural use and carbon sequestration presents a significant challenge. The total mass of organic residues produced annually in wastewater, animal manure, forestry, and crop residues (after deducting 30% of the total crop residues that must be retained in the soil) is estimated globally at over 7.3 billion tonnes [34].

Artisanal biochar production is scarcely addressed in the scientific literature, particularly regarding small-sized biomass (most agricultural residues are small-sized). This is likely due to the considerable complexity involved, which encompasses numerous variables, especially in the initial two phases of biochar systems: the biomass used as raw material and the conversion processes. This lack of research underscores the need for innovative, decentralised, and cost-effective solutions for isolated rural areas, small-scale agriculture, and family-run farms.

In the biomass phase, variations can arise from the use of different species, drying methods, time elapsed since processing of the residue (storage method and decomposition state), separation or non-separation of different biomass parts, etc. In the artisanal thermal conversion phase, we highlight operational details of the kilns such as heat form and source, residence time, heating rates, oxygen restriction methods, complex extraction, condensation, and collection of pyrolysis gases and their byproducts, and finally, temperature monitoring and control. These issues, combined with the difficulty of scaling up artisanal production, underscore the need for further research into low-cost biochar production.

Despite all these variations, the artisanal production conducted yielded quality biochar for agricultural use and carbon sequestration, as will be demonstrated in this article. As expected, since the production of ADE likely occurred with mixtures of different biomass types, under slow, mild and uncontrolled pyrolysis, microbial and fungi metabolization and stabilisation through humification in soil [26,29,35].

The slow pyrolysis process has temperatures ranging from 250 to 750 °C, low heating rates (up to 1 °C per second), and prolonged residence time (>60 min) that favours high biochar yields, reaching of up to 45% and low yields of bio-oil and syngas [36]. The source of the biomasses [37,38], thermal conversion method, and processing [39] influence biochar characteristics. The biochar produced through slow pyrolysis can increase both soil water retention capacity and its pH, as well as the cation exchange capacity, thus increasing nutrient use efficiency [30]. This leads to enhancements in soil physical and chemical properties and greater productivity [40].

Biochar production process is usually carried out in high-tech large-scale production kilns, using complex technology and requiring large quantities of biomass for the production of biochar, which makes decentralised production unfeasible in remote tropical areas. These kilns are high in both acquisition and maintenance costs [41], have complex operations, require skilled labour, and necessitate electrical power [42], thus being inaccessible to small entrepreneurs and rural producers in the Amazon and other rural regions lacking in sustainable solutions. The seasonal availability of residues further diminishes the return on investment; therefore, the economical exploitation of this natural resource demands a low-cost approach. Moreover, research challenges include the development of mobile kilns, capable of being transported to biomass generation sites, that do not require electricity and have emission control and collection of pyrolysis by-products. The objective of this research was to develop a mobile, low-cost kiln to produce biochar from small-sized biomass as raw material that can be utilised in a decentralised manner by small rural farmers, communities, cooperatives, associations, and acai berry producers. The physicochemical and structural characteristics of the produced biochar were investigated to demonstrate the suitability of biochar for agricultural use and climate change mitigation.

2. Materials and Methods

The design and construction of a low-cost mobile pyrolysis kiln for biochar production for acai berry agro-industry waste biomass (Figure 2) were inspired by the principles of the scrum agile methodology [43]. The project was developed based on prior equipment described in the literature [9,44,45], and was directed to obtain a simple and easy to construct solution for decentralised implementation in rural areas to use and value biomass from small agro-industrial wastes.

Figure 2. (**a**) Three-dimensional schematic of the construction of the low-cost mobile pyrolysis kiln; (**b**) photograph of the kiln in operation; and (**c**) photograph pyrolysis chamber fuelled with acai berry biomass and the produced biochar.

For the production of biochar, residual biomass from acai berry agro-industries in Manaus, Amazonas state, Northern Brazil, was used as raw material. These residues consist of a mixture of fibres, seeds, pulp, and acai berry husk remnants. For biochar production, the raw material was initially sieved and then dried in an oven. The material used for carbonisation was predominantly composed of acai pits with adhering fibres. Three carbonisation processes were conducted for testing, removing residues and paints from the barrels, and adjustments to the kiln prototype. The residues were acquired, transported, dried in an oven at 105 °C for 24 h, and sieved to 2 mm to remove the fine particles from the pulp and shells.

The production of biochar from acai berry waste aimed to follow the requirements that confer more favourable agronomic conditions, namely, a residence time of 60 min between temperatures of 500 and 600 °C [18]. However, only the T1 thermocouple recorded temperatures in this range (Figure A1). The carbonisation strategy was refined with the introduction of kiln sealing using clay, drying the biomass in an oven, increasing the residence time between 300 and 499 °C, and extracting and better condensing the pyrolysis gases. These modifications ensured uniform carbonisation of the entire biomass, even with the use of the kiln's full capacity.

Of the total 18 carbonisation processes conducted to biochar production, 13 achieved 100% biomass carbonisation. Five processes were performed with incomplete carbonisation, and only the effectively carbonised biomass was considered. For the analyses presented in this article, 4 carbonisation processes were selected from the 13, considered representative of the set, covering the beginning, middle, and end of the chronological production sequence.

The four selected processes were used for the analysis of the furnace operation and for the collection of biochar samples for characterization. The selected carbonisation processes were numbers 1, 10, 16, and 17, and the four characterised biochar samples were numbered S1, S2, S3, and S4, respectively (Table A1).

This selection is justified by budgetary constraints for the analysis of biochar from all carbonisation processes. Therefore, the results presented in this article refer to these four carbonisation processes and their four produced biochar samples, unless explicitly stated otherwise.

For characterization, the biochar samples (S1 to S4) and acai berry waste were ground in a knife mill. The yield of biochar was calculated from the conversion of acai berry waste mass to biochar mass, according to Equation (1):

$$\text{yield } (\%) = (W_b/W_r)\ 100, \quad (1)$$

where W_b is the mass of biochar and W_r is the initial biomass mass (kg). The average was calculated from the data of the four sampled processes.

The pH and electrical conductivity (EC) of the biochar solution were analysed in deionised water, at a dilution of 1:20 (*w*:*v*), and maintained for 90 min under shaking in a shaker [46]; both analyses were performed in triplicate.

Thermal decomposition of biomass and biochar samples was evaluated by thermogravimetric analysis (TG), heating up to 800 °C at 10 °C·min^{-1} in an oxygen atmosphere [47]. The functional groups present in the biochar structures were identified by Fourier-transform infrared spectroscopy (FTIR), a resolution of 8 cm^{-1}, and 128 scans with a wavelength range between 4000 and 650 cm^{-1} [48].

Ash and moisture contents were obtained in laboratory muffle furnace at 750 °C for 8 h, in triplicate, with a method adapted from ASTM D1762-84 [46]. The elemental composition of carbon (C) was determined with total organic carbon (TOC), hydrogen (H) with a thermal conductivity detector (LECO), and nitrogen (N) with Kjeldahl methodology. From the contents of these elements plus ash, the oxygen (O) content was determined by difference, and atomics ratios (H/C and O/C) were calculated [49].

Carbon retention was calculated from Equation (2) [50]:

$$C_{Retention}(\%) = \frac{C_{biochar}}{C_{biomass}} \cdot Yield_{biochar}, \quad (2)$$

where $C_{biochar}$ and $C_{biomass}$ are the carbon contents of the biochar and biomass, and $Yield_{biochar}$ is the yield achieved by the biomass conversion.

The surface morphology of the biochar particles was analysed by scanning electron microscopy (SEM), with an acceleration voltage of 15 kV and magnifications of 100, 50, and 5 µm; the samples were previously coated with gold. Additionally, the surface scanning of the samples was carried out in an energy-dispersive X-ray spectroscope (EDS) for analysis of surface elements present in the porous structure of the biochars.

Mineral content (K, P, Ca, Mg, S, N, Na, Fe, Zn, Mn, Cu, Cr, B, Ni, Pb, Mo, and Cd) of the biochar samples and the raw material was determined by inductively coupled plasma optical emission spectrometry (ICP-OES). The determination of nitrogen (N) was performed by the Raney alloy method [51] and the other elements were extracted in aqua regia.

Volatile matter was calculated by the difference between the initial and final mass of the TG analysis, discounting the moisture content. The fixed carbon content was determined by subtracting the total moisture, ash, and volatile matter from 100% [52]. The thermostable fraction (TSF) of biochar was defined as the ratio of fixed carbon to the sum of volatile matter [53], according to Equation (3).

$$TSF(\%) = \frac{\text{Fixed carbon}}{\text{Volatile matter} + \text{Fixed carbon}} \cdot 100, \quad (3)$$

3. Results and Discussion

3.1. Kiln Construction and Biochar Production

The kiln was constructed with metal barrels and a casting kiln reused from industries in the Manaus Free Trade Zone, Amazonas state, Brazil. The pyrolysis kiln consists of an insulating compartment, pyrolysis chamber, gas extraction tube, condenser, refractory kiln base, and accessories (Figure 2). The insulating compartment was constructed from two 200 L metal barrels, with an external diameter of 580 mm, height of 845 mm, and thickness of 1 mm. One of the barrels was bisected lengthwise and welded with a reduced opening in 25 mm, creating a dual wall that was packed with a 25 mm thick layer of ceramic fibre blanket for thermal insulation. Carbon steel discs of 3 mm were used as the lid and base of the compartment.

The pyrolysis chamber was constructed from a 100 L metal barrel, with dimensions of 445 mm in diameter, 690 mm in height, and 1.5 mm in thickness. A 3 mm carbon steel disc was welded to the base of the pyrolysis chamber, along with carbon steel tubes to improve heat distribution to the biomass. An atmospheric burner with a maximum power of 12.8 KW^2 was used as the heat source, due to the need for greater control of temperature and residence time, with less labour required compared to the use of wood. This burner was powered by a 13 kg residential liquefied petroleum gas (LPG) cylinder and installed on a kiln base constructed with 3 mm ironsteel plates and 75% alumina refractory bricks, previously used in aluminium casting.

The gases resulting from carbonisation were collected by a 3 m long metal extraction tube, which enabled partial condensation. To assess the temperature of the pyrolysis process, 40 cm thermocouples (mineral insulation penetration type K) were installed at 21 cm from the top (T1) and 17 cm from the base (T2) of the pyrolysis compartment and connected to a two-channel thermometer with a data logger. Temperature control was carried out by controlling the flame (gas and oxygen mixture) and sealing the furnace interfaces with clay.

In each carbonisation process, the pyrolysis chamber was loaded with the biomass, closed, sealed with clay, and placed inside the insulating compartment, which in turn was closed and positioned over the refractory brick kiln manually (Figure 2a). The insulating

compartment was sealed with clay, both on the lid and at the interface with the refractory brick, and the thermocouples were installed.

The gas exhaust tube was connected above the pyrolysis compartment lid. The thermometer was then set up for data acquisition, the atmospheric burner was turned on, adjusted for a stable flame (regulating the gas and oxygen ratio), and positioned inside the refractory brick kiln cavity.

The temperature ranges, average residence times, and heating rates (calculated every three minutes) are presented in Table 1. The biochar produced was maintained for an average of 145 min at a mean temperature between the two thermocouples of 431.7 °C. The average of the thermocouples was selected as it more accurately represents the material produced.

Table 1. Temperature ranges; average heating rate, calculated every 3 min; temperature; and residence time.

Temperature Range (°C)	Mean		
	Maximum Heating Rate (°C min^{-1})	Temperature (°C)	Residence Time (min)
25–119	4.1	84.6	122.6
120–249	6.5	171.8	76.8
250–349	5.5	305.8	31.0
350–600	3.2	436.9	162.0

The maximum mean temperature was 553.3 °C and the atmospheric burner remained on for 6 h on average. After the T1 thermocouple reached a residence time of 60 min above 500 °C, the atmospheric burner was turned off, the remaining kiln openings were sealed with clay, and cooling occurred naturally. The pyrolysis temperature was recorded until it showed a constant declining trend, so the information in Table 1 is representative up to this point and the time spent in the last temperature range is underestimated and the average temperature is approximate. The biochar was removed from the pyrolysis chamber, weighed, ground in a knife mill, and sieved to a particle size of up to 2 mm.

Approximately 190 kg of biochar was produced from 750 kg of acai waste biomass in 18 pyrolysis processes, an average of 42 kg of carbonised acai waste per batch. Biochar was used in agronomic experiments in greenhouses and in the field. Appendix A includes details of each of the four sampled carbonisation processes: Table A1—some details; Table A2—descriptive statistics; Figure A1—temperature curves by temperature range and thermocouples.

The kiln developed in this study produced an average of 13.3 kg of biochar per batch, with an average yield of 27.8% and an average fuel consumption of 4 kg of LPG gas per batch (S1 and S2). The yield of this project is within the expected range for wood or lignocellulosic biomasses [54]. This result was close to that found by Sato et al., 2020, who reported a yield of 27.81% for acai berry waste biomass using a manual pyrolysis kiln with an average temperature of 300 °C, a maximum of 450 °C, and a residence time of 9 h. A maximum yield of 25.4% at 400 °C was reported for acai biomass using a muffle-type furnace [17].

A review article on different low-cost kilns presents results similar to the kiln in this project [55]. The most comparable models are drum kilns, but with quite significant differences in design and operation. The kiln in this project uses an external heat source, meaning that the biomass itself does not combust to drive the carbonisation process. In general, small-sized lignocellulosic biomasses present carbonisation challenges compared to woods. Other differences include the insulation compartment, which protects the operator and helps restrict oxygen, and a refractory brick base for the use of the atmospheric burner. In terms of biochar productivity, we achieved nearly 28%, whereas the values presented in the review for drum kilns range from 10 to 39% [55]. Another study reports that the average biochar productivity under the slow pyrolysis process is between 15–32% for this type of biomass [54].

Producing biochar from acai berry waste proved to be a labour-intensive process due to the moisture and composition of the raw material and the carbonisation processes. Although cooking gas offers significant advantages such as reduced labour and enhanced control over the pyrolysis process, which affects the characteristics of the biochar, choosing renewable energy sources is crucial to realise its climate mitigation potential. The main challenges in producing biochar from acai berry waste were (1) the need for prior drying of the biomass; (2) establishment of a carbonisation protocol; (3) condensation of volatile gases and collection of pyrolysis byproducts.

3.2. Approximate Analyses

Throughout the four carbonisation processes, we observed a gradual increase in fixed carbon, reduction in moisture, and volatile material compared to the raw material (Figure 3). Comparing the average results of the biochar with the raw material, we observed an average increase of 49% in fixed carbon content, 3.3% in ash content, and average reductions of 46.9% in volatile matter and 5.6% in moisture. The low ash content possibly results from moderate temperatures of slow pyrolysis, with effective conversion of volatile components into more stable forms, resulting in a recalcitrant biochar with carbon sequestration capacity [36,56].

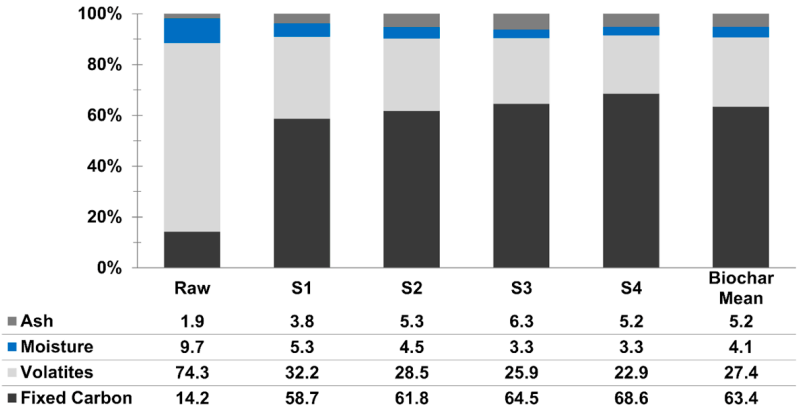

	Raw	S1	S2	S3	S4	Biochar Mean
Ash	1.9	3.8	5.3	6.3	5.2	5.2
Moisture	9.7	5.3	4.5	3.3	3.3	4.1
Volatites	74.3	32.2	28.5	25.9	22.9	27.4
Fixed Carbon	14.2	58.7	61.8	64.5	68.6	63.4

Figure 3. Approximate characterization of fresh biomass (raw) and the four biochar samples (S1 to S4) produced with the pyrolysis kiln. Samples in chronological order of pyrolysis.

The fixed carbon results were very similar to those obtained by Sato et al. (2020) of 62.48%, who also used acai berry waste to produce biochar in a homemade pyrolysis kiln. Meanwhile, the results for volatile matter and ash were slightly different, at 34.7% and 2.8%, respectively [9]. Compared with Dias et al. (2019), mean volatile matter was compatible with acai biochar produced between 500 and 600 °C and our mean ash results are a little superior [17]. The variations observed between the biochar samples can be justified by the adjustments introduced in the carbonisation processes specified in Sections 2 and 3.1. The average TSF of the biochar samples was 69.9%, which represents a thermostable fraction higher than Adhikari et al. (2024), who reported 60% for biochar produced from more than one type of woody or grassy biomass in simple pyrolysis [53].

3.3. Elemental Analysis

The thermal conversion retained about 91.8% of the C and reduced 45% of H compared to the biomass. The average atomic H/C ratio of the biochar samples was 0.55, showing a reduction of about 74% compared to the raw material (Table 2). This suggests that 50% of the carbon present in this biochar is likely to remain in the soil for approximately 100 years [57].

Comparing the results of this study with those of Dias et al. (2019), we find that the average contents of C, H, pH, and H/C and O/C ratios are compatible with acai biochar produced above 500 °C. The atomic H/C ratio in this study classifies the material as biochar, being below 0.7 [46], and 69% lower (0.74) than that reported by Sato et al. (2020). Lower

H/C ratio is likely associated with the higher temperatures achieved in this study, which produced a more recalcitrant biochar [54]. The mean O/C ratio lower than 0.2 appears to provide a 1000-year biochar half-life in soil [58]. The International Biochar Initiative (IBI) Biochar Classification Tool estimates mainly with H/C ratio that 538 g kg^{-1} of the biochar from this study should remain in the soil for at least 100 years, corresponding to Carbon Storage Class 4 [59]. There is only one carbon storage class higher than 4, which is class 5, with more than 600 g kg^{-1} stable for over 100 years.

Table 2. Characterization of fresh biomass and average of the four biochar samples produced with the pyrolysis kiln, with standard deviation (SD) and standard error (SE) information.

Element	Unit	Raw	Sample				Biochar Mean	95% Confidence Interval		Standard Deviation
			S1	S2	S3	S4		Lower Limit	Upper Limit	
Carbon (C)	%	83.79	79.57	72.31	78.05	77.92	76.96	71.89	82.03	3.189
Hydrogen (H)		2.69	1.29	1.58	1.52	1.48	1.47	1.27	1.67	0.125
Nitrogen (N)		0.24	0.32	0.37	0.59	0.36	0.41	0.21	0.60	0.122
Oxygen (O)		11.44	15.00	20.48	13.58	15.08	16.04	11.20	20.87	3.041
H/C	Molar ratio	0.38	0.19	0.26	0.23	0.23	0.23	0.19	0.27	0.028
O/C		0.10	0.14	0.21	0.13	0.15	0.16	0.10	0.22	0.037
C Retention	%	-	25.84	24.05	26.91	25.44	25.56	23.68	27.44	1.183
pH (H_2O)	-	5.58	9.21	7.77	9.18	9.28	8.86	7.70	10.02	0.728
EC	$\mu S\ m^{-1}$	687	183	259	292	358	273	157.22	388.78	72.760

The C Retention content from the conversion process, an indicator of the carbon sequestration potential of biochar, confirms that the produced biochar is slightly less stable with an average of 25.56%, compatible with temperatures between 400 and 500 °C [50]. It was found that the carbon stability of biochar is primarily associated with the type of feedstock, and that biochar produced via a simple pyrolysis method exhibits structural stability comparable to biochar produced from advanced pyrolysis methods [53].

3.4. pH and EC

The pH and EC of the samples in this study showed substantial changes in chemical properties when compared to biomass (Table 2). The biochar had a pH range between 7.77 and 9.28, qualifying it as having a basic average pH of 8.86. The lower pH value observed in sample S2 may be related to the use of the maximum capacity of the pyrolysis compartment in that carbonisation process, around 57 kg of biomass—see Table A1. The pH results were notably higher than those reported in another study, which showed a pH of 5.73 for biochar from acai berry waste produced at an average temperature of 300 °C [9]. The thermal conversion carried out likely caused the decomposition of organic materials and the disappearance of acidic functional groups such as –COOH and –OH in the biochar [60].

For the biochar, the average electrical conductivity (EC) was 273 $\mu S \cdot m^{-1}$, representing a reduction of 60% after the carbonisation process (Table 2). Biochar influences the interaction of electrons that dominate the exchange processes between the environment and soil nutrients, thereby affecting soil fertility and quality [61]. It was found that the electrical conductivity of biochar from different biomasses increased with the pyrolysis temperature, while the heating rate and the type of raw material only marginally affected electrical conductivity [62].

The pH and EC parameters affect nutrient availability in the soil and can be influenced by biochar [61]. Especially in acidic soils, the incorporation of alkaline biochar reduces acidity, increases the availability of cations, and reduces Al+3 and H+ ions, resulting in an increase in base saturation [63]. Acai berry biochar stands out as a potential amendment for acidic Amazonian soils and can contribute to increasing their fertility and reducing costs with mineral inputs.

3.5. Inorganic Matter

Results demonstrate the presence of essential elements for plant growth and development with a significant rate for the element K, but also noteworthy for P, Ca, Mg, S, and N (Table 3). The most significant micronutrients in the evaluated samples were Fe, Mn, Zn, Cr, and B.

Table 3. Results of inorganic matter analysis of the biochar samples obtained from ICP analysis.

Element	Raw	Biochar Sample (g/kg Dry Matter)						CI 95%	
		S1	S2	S3	S4	Mean	SD	Lower Limit	Upper Limit
K	3.73	5.79	8.89	9.77	10.27	8.68	2.0093	5.48	11.88
P	0.97	1.58	1.94	2.34	2.60	2.12	0.44822	1.40	2.83
Ca	0.88	1.33	1.37	1.76	1.58	1.51	0.1995	1.19	1.83
Mg	0.81	0.90	1.37	1.62	1.77	1.42	0.38092	0.81	2.02
S	0.19	0.41	0.70	0.64	0.57	0.58	0.1252	0.38	0.78
Na	0.13	0.22	0.07	0.07	0.04	0.10	0.0812	−0.03	0.23
Fe	0.1875	0.6877	1.1875	0.9270	0.7654	0.8919	0.2208	0.5405	1.2433
Zn	0.0114	2.1044	0.0199	0.0251	0.0235	0.5432	1.0408	−1.1129	2.1994
Mn	0.0690	0.1173	0.1482	0.1525	0.2016	0.1549	0.0349	0.0994	0.2104
Cu	0.0069	0.6279	0.0100	0.0140	0.0099	0.1655	0.3083	−0.3251	0.6560
Cr	0.0034	0.0077	0.0188	0.0147	0.0206	0.0155	0.0057	0.0063	0.0246
B	0.0041	0.0180	0.0131	0.0125	0.0110	0.0137	0.0030	0.0088	0.0185
Ni	0.0030	0.0051	0.0074	0.0056	0.0091	0.0068	0.0018	0.0039	0.0097
Pb	0.0004	0.0054	0.0017	0.0018	0.0016	0.0026	0.0019	−0.0003	0.0056
Mo	0.0003	0.0014	0.0007	0.0007	0.0007	0.0009	0.0004	0.0003	0.0014
Cd	0.0000	0.0002	0.0001	0.0001	0.0001	0.0001	0.0001	0.0000	0.0002

Among some metallic components, we observed indications of possible contamination of the produced biochar, since they were not present in the raw material in a significant way and the concentration decreased in subsequent carbonisation processes. The concentrations of copper (Cu), Zn, and lead (Pb) are high in sample S1, followed by a marked reduction from sample S2. These elements are commonly used in carbon–steel alloys and in the anti-corrosive materials in the coatings of the drums that were reused in the construction of the pyrolysis kiln. The concentration of Fe which may be related to the oxidation of the kiln's metallic components due to high temperatures or variations in the biomass used as raw material.

The biochar produced in this study can contribute to the nutrient supply in the soil, without the risk of soil salinisation from elements such as potassium (K) and sodium (Na), which are not present in high concentrations in this biochar.

Potentially hazardous elements (PHEs) such as cadmium (Cd) and lead (Pb) are present in low concentrations, while chromium (Cr) appears at a concentration approximately three times higher than that reported for tobacco seed residues [64]; however, the levels of all elements identified in the biochar samples are within the margin of safety [46].

3.6. Morphological Analysis

Scanning electron microscopy (SEM) reveals indications of the irregular rough peripheral surface morphology of the biochar particles (Figure 4); no significant variations among the samples were identified. The 5 µm image represents the interior of the central deformation shown in the 50 µm image. This rough surface is a consequence of the carbonisation process temperature. The empty spaces on the surface of the healthy structure are capable of retaining water even in conditions of low soil humidity, thus creating humid sites [65].

The elemental analysis provided by SEM-EDS presents semi-quantitative results of the elements present on the surface of the biochar. The results for all samples (Table 4) showed a chemical composition of higher amounts of C and lower amounts of inorganic elements, such as Ca, Fe, K, and Nb. The carbon content increased as the carbonisation processes were improved, except for sample S2, which shows a lower content than S1, confirming the data and analyses presented in Table 2.

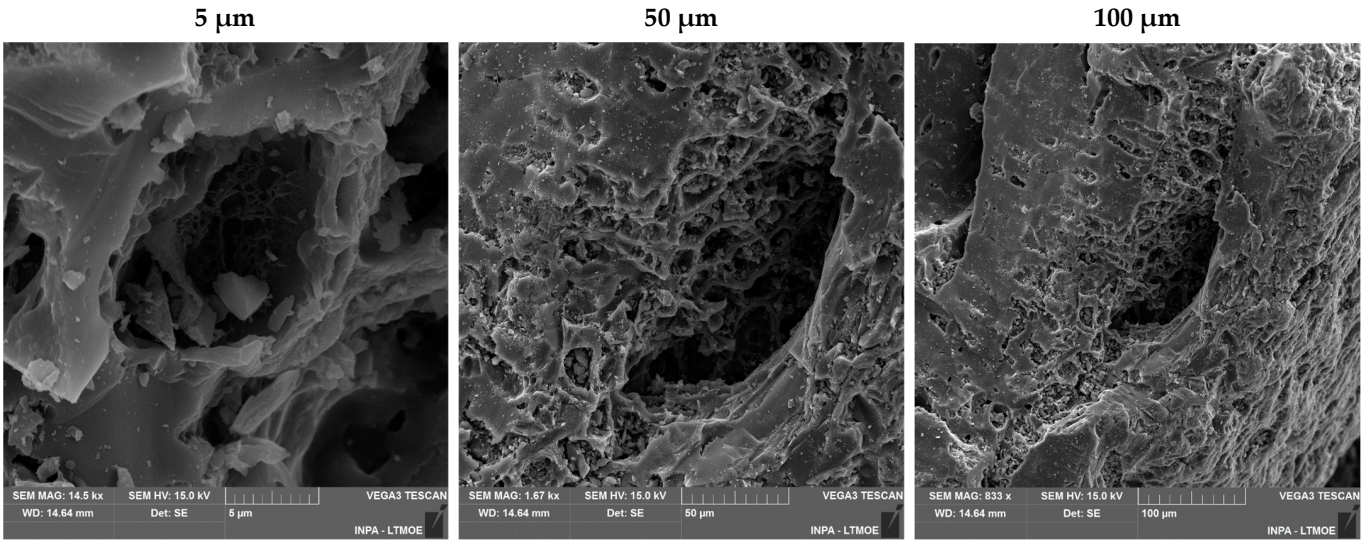

Figure 4. Scanning electron microscopy of biochar particles produced with magnifications of 5, 50 and 100 µm of S4.

Table 4. Result of EDS analysis of four biochar samples.

Sample	Elements (Mass %)					
	C	O	Ca	Fe	K	Nb
S1	83.83	15.45	0.09	0.02	0.6	0.02
S2	76.29	22.77	0.11	0.01	0.75	0.08
S3	97.45	-	0.17	0.02	1.55	0.81
S4	99.06	-	0.18	0.08	0.63	0.02
Mean	89.16	-	0.14	0.03	0.88	0.23

3.7. Thermal Decomposition

Thermogravimetric analysis of fresh biomass and biochar samples was used to estimate the decomposition profile. From the TG-DTG curves, three stages of mass loss for the fresh biomass sample were observed. The first loss occurred between 30 and 187 °C and is related to a mass loss of 9.70%, probably referring to dehydration, up to around 120 °C, and volatile compounds present in the sample. The second loss between 187 and 400 °C was 60.99%; this temperature range is known as the active pyrolysis zone. This is due to the devolatilization of hemicellulose and cellulose. The third region from 400 to 800 °C refers to the slow decomposition of lignin, with a mass loss of 11.5% (Figure 5).

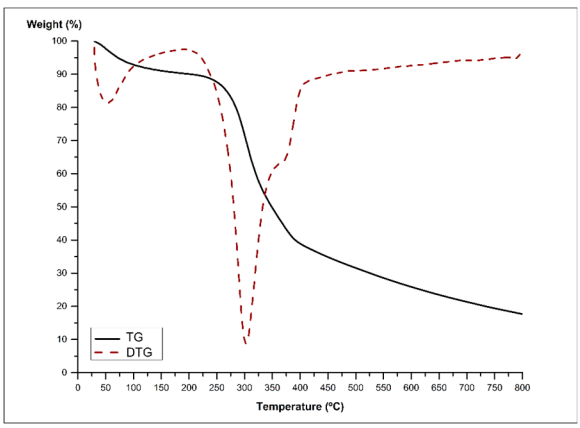

Figure 5. TG and DTG of fresh biomass.

The temperature ranges were similar to those reported in another study which also analysed acai berry biomass, while the mass loss results were slightly different at 6% (between 30 and 187 °C), 44% (between 187 and 410 °C), and 21.6% (above 400 °C) [19]. Possibly, these differences result from the sample preparation, for example, the complete separation of fibres attached to acai berry seeds, not performed in this study.

In the scientific literature, variability in the reported composition of acai berry biomass can be observed, which may be attributed to the diverse methodologies employed in its analysis A holocellulose content (hemicellulose + cellulose) of 40% and lignin content of 41% have been reported [19]. Meanwhile, cellulose levels of 8.5%, hemicellulose of 48.1%, and lignin of 16.4% have been reported in another study [66]. In general, in lignocellulosic biomasses, hemicellulose is degraded between 200 and 350 °C, cellulose between 300 and 430 °C, and lignin between 250 and 550 °C [67].

The fresh biomass lost about 82% of its initial mass upon reaching 800 °C. Meanwhile, the four biochar samples lost on average 28.54% of their initial mass. Figure 6 represents the TG-DG curves for the biochar samples. This thermodecomposition profile shows two stages of mass loss. The first mass loss between the initial temperature up to 120 °C is related to the evaporation of water and/or partial degradation of light organic compounds. The second mass loss was recorded from 200 °C and occurred due to the decomposition of carbon-based material.

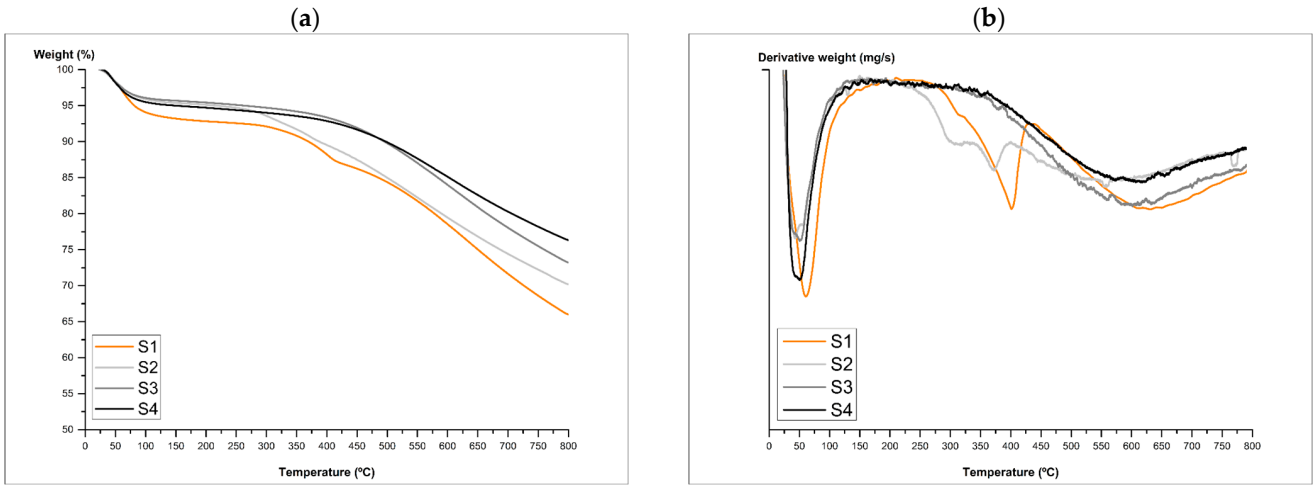

Figure 6. TG analysis (**a**) and DTG (**b**) for the four biochar samples.

The first burns in the pyrolysis kiln were from sample S1 show stages of decomposition more similar to fresh biomass. Sample S1 lost 33.98% of its initial mass, while sample S4 lost 23.61%, a difference of only 10.37%. The greater stability of the last carbonisation processes, S2 and S3, is probably due to the increase in residence time above 300 °C, since this strategy may have increased the degradation of the main components of lignocellulosic biomass.

3.8. Functional Groups

The FTIR spectra show a reduction in the intensity of peaks in the region from 1500 to 1100 cm^{-1} compared to the peaks in the same region of the raw material (Figure 7). In the biochar samples' spectra, four main peaks are observed at 2160, 2025, 1970, and 910 cm^{-1}, which are characteristic of the bonds present in aromatic hydrocarbons such as C=C, C−H, C=O, and C−H, respectively. These peaks become more intense compared to the raw sample, due to the development of the biochar structure during the pyrolytic process.

The band present between 3000 and 3500 cm^{-1} represents moisture absorption, characteristic of the −OH bond, which decreases in intensity during the pyrolysis process. The disappearance of the characteristic −OH band after pyrolysis does not influence the structure of the biochar. It is expected that this band will be absent or of lower intensity after the carbonisation process, as it is conducted at high temperatures, reducing the sample's

moisture content. The moisture content in the sample can be assessed by the intensity of the −OH band. According to the literature, this is predictable due to the cracking of phenolic–aromatic structures performed by the pyrolysis process [68]. The peak observed at 2920 cm^{-1} indicates the C−H bond also present in the aliphatic structures (C−H) of the raw material, not present in biochar samples.

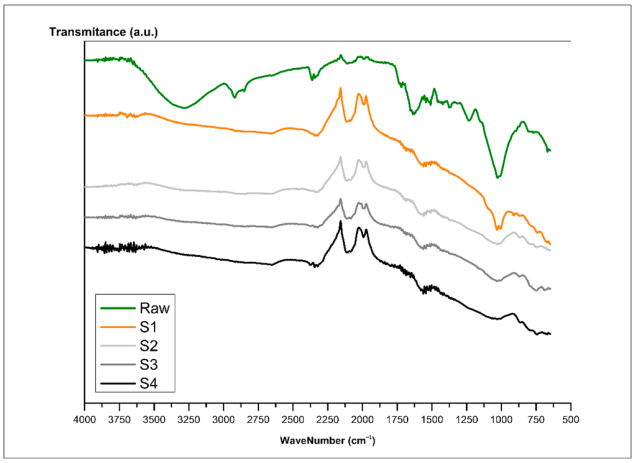

Figure 7. FTIR analysis performed for the biomass and four samples of produced biochar.

The degradation of aliphatic compounds is related to the reduction of biochar's hydrophobicity, leading to the disappearance of bands at 2920 and 2850 cm^{-1} at high pyrolysis temperatures, between 500 and 700 °C [69], which can be observed for samples S1, S2, and S3. This characteristic is important for agricultural use due to the potential increase in water retention capacity.

The peaks at 1570 and 1480 cm^{-1} for the raw material are related to the presence of secondary amines and amides (N−H). After the thermal conversion of biomass, these groups were reduced. The peak at 1570 cm^{-1}, representing C=C, was found to reduce with an increase in temperature [17].

The peaks at 1030 and 1005 cm^{-1}, identified with more intensity in the raw material and in sample S1, are related to the presence of alcohol and ether functional groups, whereas in samples S2, S3, and S4, the pyrolysis was possibly more efficient and contributed to the greater thermal degradation of these groups, with monitoring on the heating ramps and more extended retention time on each ramp. Moreover, the vibrations at 840 and 790 cm^{-1} are associated with out-of-plane C−H (R2C=CHR), which was clearer in the raw material and was reduced in the biochar samples.

3.9. Correlations

A correlation matrix is available in Table A3. Electrical conductivity (EC) was negatively correlated with volatiles and positively correlated with fixed carbon and "Time above 250 °C", as expected from the literature [70]. "Time above 250 °C" was also correlated with fixed carbon, which depends on temperature and, primarily, on the type of biomass [52]. It showed a negative correlation with volatiles and moisture, whose contents inevitably decline with increasing temperatures and pyrolysis time.

Carbon content was strongly positively correlated with pH, both benefiting from improved carbonisation, unlike oxygen content, which was negatively correlated with pH. The positive correlation between moisture content and "Average temperature above 250 °C" may result from improved sealing of the kiln during the carbonisation processes. Enhanced oxygen restriction in the pyrolysis chamber led to lower temperatures, compensated by a longer residence "Time above 250 °C". As a result, the biochar was produced more uniformly and exhibited improved parameters for material stability (fewer volatiles) and agricultural use (pH). This reinforces that these variations do not compromise the benefits that the produced biochar can provide for agronomic and climate change use.

4. Conclusions

Acai berry wastes are some of the most abundant agro-industrial wastes in the Amazon region, considered an environmental liability, that can be used for biochar production. The biochar produced with 145 min of residence time and 431.7 °C average presented favourable characteristics for agronomic use (with basic pH and nutrients) and carbon sequestration in the soil. Even with the variations inherent in artisanal production, the biochar produced exhibits favourable characteristics for agronomic use and climate change mitigation.

The characterisation of inorganic elements in the biochar demonstrated that caution is necessary with the use of kilns designed with low-resistance metallic components. The high rates of Fe, Zn, and Cu in some samples indicate the possibility of these elements being released at high temperatures, requiring monitoring to avoid soil and plant depletion. No high levels of potentially hazardous elements (PHEs) in the produced biochar were verified in this study.

Therefore, attention is needed for the rates and frequency of biochar application, as is carried out with agricultural inputs, to reduce the possibility of soil salinization and contamination. There is a gap in the literature regarding the design of medium-sized, mobile artisanal kilns that can be replicated for small-sized biomass to achieve certain productive uniformity and operational safety. These designs should include the use of materials inert at high temperatures in the construction of the kiln, such as stainless steel and refractory bricks, and propose solutions to the complex issue of condensation systems and collection of pyrolysis byproducts.

Author Contributions: V.J.: Conceptualization, Methodology, Investigation, Writing, Funding acquisition; A.R.d.O.B.: Writing, Reviewing, Funding acquisition; C.K.A.d.O.D.: Project administration; H.M.S.: Investigation, Methodology, Reviewing; F.E.D.: Investigation; R.O.d.A.: Methodology, Reviewing; C.S.d.C.M.-d.-S.: Supervision, Reviewing; N.P.d.S.F.: Supervision; J.F.C.G.: Supervision. All authors have read and agreed to the published version of the manuscript.

Funding: This work was funded by the Amazonas State Research Foundation (Fundação de Amparo à Pesquisa do Estado do Amazonas—FAPEAM) through Notice Number 001/2021—Women in Science, Process Number 01.02.016301.01742/2021.

Data Availability Statement: All data are available and can be provided upon request.

Acknowledgments: The authors express deep gratitude for the support received at all stages of this research from the Federal Institute of Education of Amazonas (IFAM—Brazil), the National Institute of Amazonian Research (INPA—Brazil). FCT—Fundação para a Ciência e Tecnologia, I.P. by project reference UIDB/00239/2020 of the Forest Research Centre, DOI 10.54499/UIDB/00239/2020, and LA/P/0092/2020 of Associate Laboratory TERRA, DOI 10.54499/LA/P/0092/2020. Finally, we express our gratitude to the Doctoral Program in Climate Change and Sustainable Development Policies, the Institute of Social Sciences of the University of Lisbon (ICS-UL), and the School of Agriculture (ISA-UL).

Conflicts of Interest: The authors declare no conflicts of interest.

Appendix A

Table A1. Details of the four carbonisation processes representative of biochar production that gave rise to the characterised biochar samples.

Sample	Carbonisation Process Number	Biomass (kg)	Biochar (kg)	Gas (kg)	Maximum Temperature (°C)		Total Carbonisation Time (min)
					Thermocouple T1	Thermocouple T2	
S1	1	37.8	10.3	4.4	548.6	561.6	351
S2	10	57.4	16.0	5.6	590.3	433.3	375
S3	16	45.0	13.0	2.8	567.7	425.2	351
S4	17	47.3	12.9	3.3	570.8	405.6	400

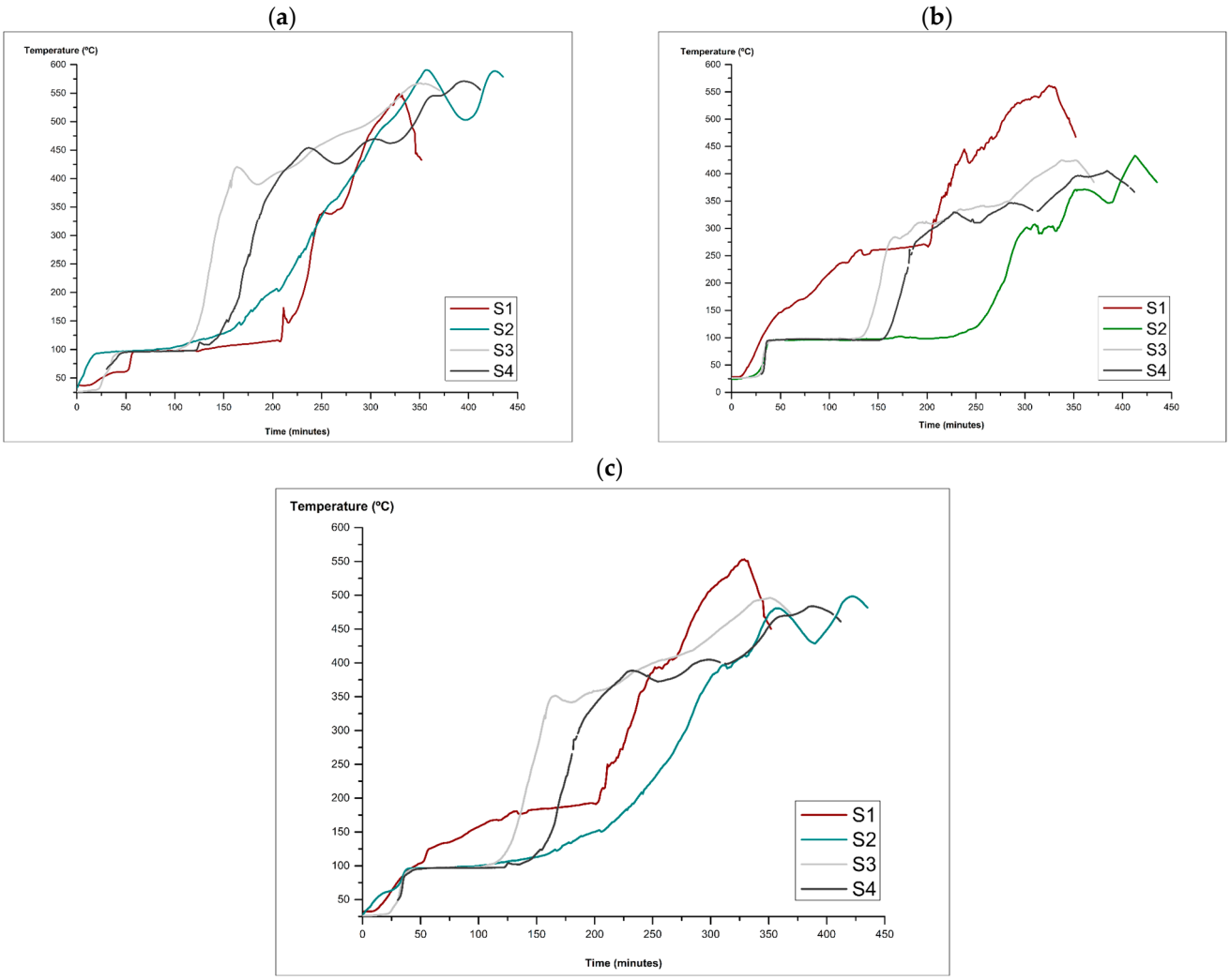

Figure A1. Temperature curves of the four carbonisation processes in thermocouples T1 (**a**), T2 (**b**), and (**c**) mean temperatures between T1 and T2.

Table A2. Descriptive statistics of the four carbonisation processes representative of biochar production that gave rise to the characterised biochar samples.

	95% Confidence Interval			
	Mean	**Lower Limit**	**Upper Limit**	**Standard Deviation**
Biomass (kg)	46.89	34.03	59.75	8.081
Biochar (kg)	13.06	9.35	16.77	2.329
Yield (biochar/biomass−%)	27.83	26.62	29.04	0.759
Gas consumption (kg)	4.04	2.05	6.02	1.249
Total carbonisation time (min)	392.38	332.06	452.69	37.906
Time above 250 °C (min)	193	122.54	263.46	44.279
Average temperature above 250 °C (°C)	415.93	393.54	438.33	14.074
Average maximum temperature (°C)	507.94	458.79	557.09	30.889

Note. The CI of the mean assumes that the sampling distribution of the mean follows a t-distribution with N-1 degrees of freedom.

Table A3. Correlation matrix of variables from four biochar samples.

	Total Carbonisation Time (min)	**Time above 250 °C (min)**		**Average Temperature above 250 °C**		**Average Maximum Temperature (°C)**	**Moisture (%)**	**Ash (%)**	**pH (H_2O)**		**Electrical Conductivity**		**C**	**N**	**O**	**H**	**Volatiles**		**Fixed C**
Total carbonisation time (min)	—																		
Time above 250 °C (min)	0.306	—																	
Average temperature above 250 °C	−0.499	−0.963	*	—															
Average maximum temperature (°C)	−0.698	−0.884		0.969	*	—													
Moisture (%)	−0.288	−0.995	**	0.971	*	0.885	—	—											
Ash (%)	0.301	0.789		−0.873		−0.804	−0.844												
pH (H_2O)	−0.717	0.288		−0.023		0.183	−0.256	−0.100	—										
Electrical conductivity	0.518	0.950	*	−0.934		−0.922	−0.922	0.643	0.161		—								
C	−0.851	0.038		0.227		0.428	−0.011	−0.285	0.966	*	−0.097		—						
N	−0.205	0.556		−0.570		−0.408	−0.632	0.862	0.164		0.289		0.068	—					
O	0.770	−0.344		0.103		−0.133	0.339	−0.097	−0.962	*	−0.145		−0.926	−0.413	—				
H	0.770	0.569		−0.769		−0.853	−0.608	0.814	−0.605		0.585		−0.771	0.460	0.482	—			
Volatiles	−0.450	−0.972	*	0.943		0.910	0.948	−0.674	−0.220		−0.996	**	0.038	−0.354	0.219	−0.564	—		
Fixed C	0.416	0.951	*	−0.899		−0.864	−0.916	0.588	0.289		0.991	**	0.035	0.273	−0.260	0.474	−0.993	**	—

Note: * $p < 0.05$, ** $p < 0.01$.

References

1. CONAB. *Boletim da Sociobiodiversidade*; Companhia Nacional de Abastecimento: Brasília, DF, Brazil, 2022.
2. IBGE. Produção Agrícola Municipal (PAM 2021). Available online: https://sidra.ibge.gov.br/tabela/1613 (accessed on 12 July 2023).
3. IBGE. Produção da Extração Vegetal e da Silvicultura (PEVS 2021). Available online: https://sidra.ibge.gov.br/pesquisa/pevs/quadros/brasil/2021 (accessed on 12 July 2023).
4. Tavares, G.d.S.; Homma, A.K.O.; de Menezes, A.A.; Palheta, M.P. Análise da Produção e Comercialização de Açaí no Estado do Pará, Brasil. In *Sinergias de Mudança da Agricultura Amazônica: Conflitos e Oportunidades*; Homma, A.K.O., Ed.; Embrapa: Brasília, DF, Brazil, 2022; pp. 444–463.
5. Laurindo, L.F.; Barbalho, S.M.; Araújo, A.C.; Guiguer, E.L.; Mondal, A.; Bachtel, G.; Bishayee, A. Açaí (*Euterpe oleracea* Mart.) in Health and Disease: A Critical Review. *Nutrients* **2023**, *15*, 989. [CrossRef]
6. IBGE. Produção de Açaí (Cultivo) No Brasil. Available online: https://www.ibge.gov.br/explica/producao-agropecuaria/acai-cultivo/br (accessed on 12 January 2024).
7. Bufalino, L.; Guimarães, A.A.; Silva, B.M.d.S.e.; de Souza, R.L.F.; de Melo, I.C.N.A.; de Oliveira, D.N.P.S.; Trugilho, P.F. Local Variability of Yield and Physical Properties of Açaí Waste and Improvement of Its Energetic Attributes by Separation of Lignocellulosic Fibers and Seeds. *J. Renew. Sustain. Energy* **2018**, *10*, 053102. [CrossRef]
8. Batista, J.G.; Correa, L.P. *Destinação do Resíduo de Açaí em um Supermercado de Capanema-PA e a Redução de Emissões de Metano*; Universidade Federal Rural da Amazônia: Capanema, PA, USA, 2021.
9. Sato, M.K.; de Lima, H.V.; Noronha Costa, A.; Rodrigues, S.; Mooney, S.J.; Clarke, M.; Silva Pedroso, A.J.; de Freitas Maia, C.M.B. Biochar as a Sustainable Alternative to Açaí Waste Disposal in Amazon, Brazil. *Process Saf. Environ. Prot.* **2020**, *139*, 36–46. [CrossRef]
10. de Castro, D.A.R.; Da Silva Ribeiro, H.; Hamoy Guerreiro, L.; Pinto Bernar, L.; Jonatan Bremer, S.; Costa Santo, M.; Da Silva Almeida, H.; Duvoisin, S.; Pizarro Borges, L.; Teixeira Machado, N. Production of Fuel-Like Fractions by Fractional Distillation of Bio-Oil from Açaí (*Euterpe oleracea* Mart.) Seeds Pyrolysis. *Energies* **2021**, *14*, 3713. [CrossRef]
11. Mares, E.K.L.; Gonçalves, M.A.; Da Luz, P.T.S.; Da Rocha Filho, G.N.; Zamian, J.R.; Da Conceição, L.R.V. Acai Seed Ash as a Novel Basic Heterogeneous Catalyst for Biodiesel Synthesis: Optimization of the Biodiesel Production Process. *Fuel* **2021**, *299*, 120887. [CrossRef]
12. Rendeiro, G. *Combustão e Gasificação de Biomassa Sólida; Soluções Energéticas para a Amazônia*, 1st ed.; Ministério de Minas e Energia: Brasília, DF, Brazil, 2008; ISBN 978-85-98341-05-7.
13. Teixeira, M.A.; Escobar Palacio, J.C.; Sotomonte, C.R.; Silva Lora, E.E.; Venturini, O.J.; Aßmann, D. Assaí—An Energy View on an Amazon Residue. *Biomass Bioenergy* **2013**, *58*, 76–86. [CrossRef]
14. Barbosa, A.d.M.; Rebelo, V.S.M.; Martorano, L.G.; Giacon, V.M. Caracterização de partículas de açaí visando seu potencial uso na construção civil. *Matéria* **2019**, *24*, e12435. [CrossRef]
15. Santos, R.K.S.; Nascimento, B.F.; De Araújo, C.M.B.; Cavalcanti, J.V.F.L.; Bruckmann, F.S.; Rhoden, C.R.B.; Dotto, G.L.; Oliveira, M.L.S.; Silva, L.F.O.; Motta Sobrinho, M.A. Removal of Chloroquine from the Aqueous Solution by Adsorption onto Açaí-Based Biochars: Kinetics, Thermodynamics, and Phytotoxicity. *J. Mol. Liq.* **2023**, *383*, 122162. [CrossRef]
16. Zaparoli, M.; Igansi, A.V.; Silveira, J.T.D.; Morais, M.G.D.; Costa, J.A.V. Biochar as a Sustainable Alternative for the Use of Residues from the Processing of Açaí and the Removal of Glyphosate. *J. Environ. Chem. Eng.* **2023**, *11*, 111162. [CrossRef]
17. Dias, Y.N.; Souza, E.S.; da Costa, H.S.C.; Melo, L.C.A.; Penido, E.S.; do Amarante, C.B.; Teixeira, O.M.M.; Fernandes, A.R. Biochar Produced from Amazonian Agro-Industrial Wastes: Properties and Adsorbent Potential of Cd^{2+} and Cu^{2+}. *Biochar* **2019**, *1*, 389–400. [CrossRef]
18. Sato, M.K.; de Lima, H.V.; Costa, A.N.; Rodrigues, S.; Pedroso, A.J.S.; de Freitas Maia, C.M.B. Biochar from Acai Agroindustry Waste: Study of Pyrolysis Conditions. *Waste Manag.* **2019**, *96*, 158–167. [CrossRef]
19. Santos, V.O.; Queiroz, L.S.; Araujo, R.O.; Ribeiro, F.C.P.; Guimarães, M.N.; da Costa, C.E.F.; Chaar, J.S.; de Souza, L.K.C. Pyrolysis of Acai Seed Biomass: Kinetics and Thermodynamic Parameters Using Thermogravimetric Analysis. *Bioresour. Technol. Rep.* **2020**, *12*, 100553. [CrossRef]
20. Li, W.; Tao, E.; Hao, X.; Li, N.; Li, Y.; Yang, S. MMT and ZrO2 Jointly Regulate the Pore Size of Graphene Oxide-Based Composite Aerogel Materials to Improve the Selective Removal Ability of Cu(II). *Sep. Purif. Technol.* **2024**, *331*, 125506. [CrossRef]
21. Zhang, J.; Yang, S.; Zhou, K.; Zhao, J.; Wang, J.; Li, N.; Wang, Y.; Li, Y.; Tao, E. Preparation of Co-Doped Biochar to Improve Electron Transfer and Modulate $^1O_2$ Generation: Unraveling the Radical-Unradical Mechanism. *Chem. Eng. J.* **2024**, *491*, 151985. [CrossRef]
22. Adegbeye, M.J.; Ravi Kanth Reddy, P.; Obaisi, A.I.; Elghandour, M.M.M.Y.; Oyebamiji, K.J.; Salem, A.Z.M.; Morakinyo-Fasipe, O.T.; Cipriano-Salazar, M.; Camacho-Díaz, L.M. Sustainable Agriculture Options for Production, Greenhouse Gasses and Pollution Alleviation, and Nutrient Recycling in Emerging and Transitional Nations—An Overview. *J. Clean. Prod.* **2020**, *242*, 118319. [CrossRef]
23. Joseph, S.; Cowie, A.L.; Van Zwieten, L.; Bolan, N.; Budai, A.; Buss, W.; Cayuela, M.L.; Graber, E.R.; Ippolito, J.A.; Kuzyakov, Y.; et al. How Biochar Works, and When It Doesn't: A Review of Mechanisms Controlling Soil and Plant Responses to Biochar. *GCB Bioenergy* **2021**, *13*, 1731–1764. [CrossRef]
24. Kumar, A.; Bhattacharya, T. Biochar: A Sustainable Solution. *Environ. Dev. Sustain.* **2021**, *23*, 6642–6680. [CrossRef]

25. Arroyo-Kalin, M. Slash-Burn-and-Churn: Landscape History and Crop Cultivation in Pre-Columbian Amazonia. *Quat. Int.* **2012**, *249*, 4–18. [CrossRef]
26. Bezerra, J.; Turnhout, E.; Vasquez, I.M.; Rittl, T.F.; Arts, B.; Kuyper, T.W. The Promises of the Amazonian Soil: Shifts in Discourses of Terra Preta and Biochar. *J. Environ. Policy Plan.* **2019**, *21*, 623–635. [CrossRef]
27. Clement, C.R.; Denevan, W.M.; Heckenberger, M.J.; Junqueira, A.B.; Neves, E.G.; Teixeira, W.G.; Woods, W.I. The Domestication of Amazonia before European Conquest. *Proc. R. Soc. B Biol. Sci.* **2015**, *282*, 20150813. [CrossRef]
28. Fraser, J.; Teixeira, W.; Falcão, N.; Woods, W.; Lehmann, J.; Junqueira, A.B. Anthropogenic Soils in the Central Amazon: From Categories to a Continuum: Anthropogenic Soils in the Central Amazon. *Area* **2011**, *43*, 264–273. [CrossRef]
29. Glaser, B.; Birk, J.J. State of the Scientific Knowledge on Properties and Genesis of Anthropogenic Dark Earths in Central Amazonia (Terra Preta de Índio). *Geochim. Cosmochim. Acta* **2012**, *82*, 39–51. [CrossRef]
30. Novotny, E.H.; Maia, C.M.B.d.F.; Carvalho, M.T.d.M.; Madari, B.E. Biochar: Pyrogenic Carbon for Agricultural Use—A Critical Review. *Rev. Bras. Ciênc. Solo* **2015**, *39*, 321–344. [CrossRef]
31. Tripathi, M.; Sahu, J.N.; Ganesan, P. Effect of Process Parameters on Production of Biochar from Biomass Waste through Pyrolysis: A Review. *Renew. Sustain. Energy Rev.* **2016**, *55*, 467–481. [CrossRef]
32. Kan, T.; Strezov, V.; Evans, T.J. Lignocellulosic Biomass Pyrolysis: A Review of Product Properties and Effects of Pyrolysis Parameters. *Renew. Sustain. Energy Rev.* **2016**, *57*, 1126–1140. [CrossRef]
33. Wiedner, K.; Glaser, B. Traditional Use of Biochar. In *Biochar for Environmental Management: Science, Technology and Implementation*, 2nd ed.; Routledge: London, UK; Taylor & Francis Group: New York, NY, USA, 2015; pp. 15–37.
34. Lefebvre, D.; Fawzy, S.; Aquije, C.A.; Osman, A.I.; Draper, K.T.; Trabold, T.A. Biomass Residue to Carbon Dioxide Removal: Quantifying the Global Impact of Biochar. *Biochar* **2023**, *5*, 65. [CrossRef]
35. Sands, B.; Machado, M.R.; White, A.; Zent, E.; Gould, R. Moving towards an Anti-Colonial Definition for Regenerative Agriculture. *Agric. Hum. Values* **2023**, *40*, 1697–1716. [CrossRef]
36. Tisserant, A.; Cherubini, F. Potentials, Limitations, Co-Benefits, and Trade-Offs of Biochar Applications to Soils for Climate Change Mitigation. *Land* **2019**, *8*, 179. [CrossRef]
37. Ippolito, J.A.; Cui, L.; Kammann, C.; Wrage-Mönnig, N.; Estavillo, J.M.; Fuertes-Mendizabal, T.; Cayuela, M.L.; Sigua, G.; Novak, J.; Spokas, K.; et al. Feedstock Choice, Pyrolysis Temperature and Type Influence Biochar Characteristics: A Comprehensive Meta-Data Analysis Review. *Biochar* **2020**, *2*, 421–438. [CrossRef]
38. Tomczyk, A.; Sokołowska, Z.; Boguta, P. Biochar Physicochemical Properties: Pyrolysis Temperature and Feedstock Kind Effects. *Rev. Environ. Sci. Biotechnol.* **2020**, *19*, 191–215. [CrossRef]
39. Zhao, B.; O'Connor, D.; Zhang, J.; Peng, T.; Shen, Z.; Tsang, D.C.W.; Hou, D. Effect of Pyrolysis Temperature, Heating Rate, and Residence Time on Rapeseed Stem Derived Biochar. *J. Clean. Prod.* **2018**, *174*, 977–987. [CrossRef]
40. Lehmann, J.; Joseph, S. (Eds.) *Biochar for Environmental Management: Science, Technology and Implementation*, 2nd ed.; Routledge: London, UK; Taylor & Francis Group: New York, NY, USA, 2015; ISBN 978-0-415-70415-1.
41. Cornelissen, G.; Pandit, N.R.; Taylor, P.; Pandit, B.H.; Sparrevik, M.; Schmidt, H.P. Emissions and Char Quality of Flame-Curtain "Kon Tiki" Kilns for Farmer-Scale Charcoal/Biochar Production. *PLoS ONE* **2016**, *11*, e0154617. [CrossRef]
42. Luo, H.; Wang, X.; Liu, X.; Wu, X.; Shi, X.; Xiong, Q. A Review on CFD Simulation of Biomass Pyrolysis in Fluidized Bed Reactors with Emphasis on Particle-Scale Models. *J. Anal. Appl. Pyrolysis* **2022**, *162*, 105433. [CrossRef]
43. Schwaber, K. *Agile Project Management with Scrum*; Microsoft Press: Redmond, WA, USA, 2004; ISBN 978-0-7356-1993-7.
44. CarbonZero. Small Scale Biochar Production. Available online: http://biochar.ch/?p=en.small_scale_biochar_kiln (accessed on 17 February 2021).
45. Sangsuk, S.; Buathong, C.; Suebsiri, S. High-Energy Conversion Efficiency of Drum Kiln with Heat Distribution Pipe for Charcoal and Biochar Production. *Energy Sustain. Dev.* **2020**, *59*, 1–7. [CrossRef]
46. *IBI-STD-2.1*; IBI Standardized Product Definition and Product Testing Guidelines for Biochar That Is Used in Soil (Aka IBI Biochar Standards), Version 2.1. International Biochar Initiative: Bowdoinham, ME, USA, 2015.
47. Leng, L.Y.; Husni, M.H.A.; Samsuri, A.W. Comparison of the Carbon-Sequestering Abilities of Pineapple Leaf Residue Chars Produced by Controlled Combustion and by Field Burning. *Bioresour. Technol.* **2011**, *102*, 10759–10762. [CrossRef]
48. Lorenz, K.; Lal, R. *Carbon Sequestration in Agricultural Ecosystems*; Springer: Cham, Switzerland, 2018.
49. Benites, V.d.M.; Mendonça, E.d.S.; Schaefer, C.E.G.R.; Novotny, E.H.; Reis, E.L.; Ker, J.C. Properties of Black Soil Humic Acids from High Altitude Rocky Complexes in Brazil. *Geoderma* **2005**, *127*, 104–113. [CrossRef]
50. Nan, H.; Yin, J.; Yang, F.; Luo, Y.; Zhao, L.; Cao, X. Pyrolysis Temperature-Dependent Carbon Retention and Stability of Biochar with Participation of Calcium: Implications to Carbon Sequestration. *Environ. Pollut.* **2021**, *287*, 117566. [CrossRef]
51. MAPA. *Manual de Métodos Analíticos Oficiais para Fertilizantes e Corretivos*; Ministério da Agricultura, Pecuária e Abastecimento. Secretaria de Defesa Agropecuária: Brasília, DF, Brazil, 2017; ISBN 978-85-7991-109-5.
52. Zhao, L.; Cao, X.; Mašek, O.; Zimmerman, A. Heterogeneity of Biochar Properties as a Function of Feedstock Sources and Production Temperatures. *J. Hazard. Mater.* **2013**, *256–257*, 1–9. [CrossRef]
53. Adhikari, S.; Moon, E.; Paz-Ferreiro, J.; Timms, W. Comparative Analysis of Biochar Carbon Stability Methods and Implications for Carbon Credits. *Sci. Total Environ.* **2024**, *914*, 169607. [CrossRef]
54. Xie, Y.; Wang, L.; Li, H.; Westholm, L.J.; Carvalho, L.; Thorin, E.; Yu, Z.; Yu, X.; Skreiberg, Ø. A Critical Review on Production, Modification and Utilization of Biochar. *J. Anal. Appl. Pyrolysis* **2022**, *161*, 105405. [CrossRef]

55. Namaswa, T.; Burslem, D.F.R.P.; Smith, J. Emerging Trends in Appropriate Kiln Designs for Small-Scale Biochar Production in Low to Middle Income Countries. *Bioresour. Technol. Rep.* **2023**, *24*, 101641. [CrossRef]
56. Lehmann, J.; Cowie, A.; Masiello, C.A.; Kammann, C.; Woolf, D.; Amonette, J.E.; Cayuela, M.L.; Camps-Arbestain, M.; Whitman, T. Biochar in Climate Change Mitigation. *Nat. Geosci.* **2021**, *14*, 883–892. [CrossRef]
57. Budai, A.; Zimmerman, A.R.; Cowie, A.L.; Webber, J.B.W.; Singh, B.P.; Glaser, B.; Masiello, C.A.; Shields, F.; Lehmann, J.; Arbestain, M.C.; et al. Biochar Carbon Stability Test Method: An Assessment of Methods to Determine Biochar Carbon Stability. *Int. Biochar Initiat.* **2013**, *1*, 1–20.
58. Spokas, K.A. Review of the Stability of Biochar in Soils: Predictability of O:C Molar Ratios. *Carbon Manag.* **2010**, *1*, 289–303. [CrossRef]
59. IBI. Biochar Classification Tool. Available online: https://biochar-international.org/resources/biochar-classification-tool/ (accessed on 4 May 2024).
60. Mukherjee, A.; Zimmerman, A.R.; Harris, W. Surface Chemistry Variations among a Series of Laboratory-Produced Biochars. *Geoderma* **2011**, *163*, 247–255. [CrossRef]
61. Sousa, E.D.T.d.S.; de Queiroz, D.M.; Coelho, A.L.d.F.; Valente, D.S.M. Development of Signal Analysis Algorithm for Apparent Soil Electrical Conductivity Sensor. *Biosyst. Eng.* **2021**, *211*, 183–191. [CrossRef]
62. Bartoli, M.; Arrigo, R.; Malucelli, G.; Tagliaferro, A.; Duraccio, D. Recent Advances in Biochar Polymer Composites. *Polymers* **2022**, *14*, 2506. [CrossRef]
63. Jemal, K. Role of Bio Char on the Amelioration of Soil Acidity. *Agrotechnology* **2021**, *10*, 212.
64. Onorevoli, B.; Da Silva Maciel, G.P.; Machado, M.E.; Corbelini, V.; Caramão, E.B.; Jacques, R.A. Characterization of Feedstock and Biochar from Energetic Tobacco Seed Waste Pyrolysis and Potential Application of Biochar as an Adsorbent. *J. Environ. Chem. Eng.* **2018**, *6*, 1279–1287. [CrossRef]
65. DeLuca, T.H.; Gundale, M.J.; MacKenzie, M.D.; Jones, D.L. Biochar Effects on Soil Nutrient Transformations. *Biochar Environ. Manag. Sci. Technol. Implement.* **2015**, *2*, 421–454.
66. Buratto, R.T.; Cocero, M.J.; Martín, Á. Characterization of Industrial Açaí Pulp Residues and Valorization by Microwave-Assisted Extraction. *Chem. Eng. Process.—Process Intensif.* **2021**, *160*, 108269. [CrossRef]
67. Jahirul, M.; Rasul, M.; Chowdhury, A.; Ashwath, N. Biofuels Production through Biomass Pyrolysis—A Technological Review. *Energies* **2012**, *5*, 4952–5001. [CrossRef]
68. Narzari, R.; Bordoloi, N.; Sarma, B.; Gogoi, L.; Gogoi, N.; Borkotoki, B.; Kataki, R. Fabrication of Biochars Obtained from Valorization of Biowaste and Evaluation of Its Physicochemical Properties. *Bioresour. Technol.* **2017**, *242*, 324–328. [CrossRef] [PubMed]
69. Zornoza, R.; Moreno-Barriga, F.; Acosta, J.A.; Muñoz, M.A.; Faz, A. Stability, Nutrient Availability and Hydrophobicity of Biochars Derived from Manure, Crop Residues, and Municipal Solid Waste for Their Use as Soil Amendments. *Chemosphere* **2016**, *144*, 122–130. [CrossRef] [PubMed]
70. Singh, B.; Dolk, M.M.; Shen, Q.; Camps-Arbestain, M. Biochar pH, Electrical Conductivity and Liming Potential. In *Biochar: A Guide to Analytical Methods*; CSIRO Publishing: Clayton, Australia, 2017; Volume 23.